

CMOS and CCD detection in Raman spectroscopy: a comparison using spontaneous and multiplex coherent anti-Stokes Raman scattering (CARS)

W.J. Niels Klement,^a Philippe Leproux,^b Wesley R. Browne,^a Hideaki Kano^c

a Stratingh Institute for Chemistry, Faculty of Science and Engineering, University of Groningen, Nijenborgh 3, 9747AG, Groningen

b Xlim research institute, University of Limoges, Limoges 87060, France

c Faculty of Science and Technology, Keio University, 3-14-1 Hiyoshi, Kohoku-ku, Yokohama, Kanagawa 223-8522, Japan

Abstract

Cooled CCD cameras are used widely in spectroscopy, mainly due to their sensitivity and low noise operating under low light conditions, and relatively high image and spectral readout rates. Despite their many advantages, CCD cameras have limitations. Particularly under bright light conditions, such as those encountered with coherent Raman spectroscopies, where the finite readout time of CCD chips is limiting. Furthermore, where weak signals need to be observed close to intense signals, blooming and smearing limit the signal to noise ratios achievable. Scientific complementary mixed oxide (sCMOS) based sensors are relatively new. Although they still show much higher readout noise than cooled CCDs, their application to spectroscopy is certainly of interest given the higher readout rates, and dynamic ranges possible. Here, we evaluate sCMOS sensors for specific spectroscopic applications, including multiplex (50 picosecond) CARS and spontaneous Raman spectroscopy. We compare the performance of a sCMOS based camera to a state-of-the-art (EM)CCD detector for these applications. The EMCCD camera outperforms the sCMOS camera in terms of limits of detection, while the sCMOS camera performs better than the CCD in terms of dynamic range and readout rate. Importantly, sCMOS camera does not suffer from interference due to blooming and smearing seen with CCD cameras, which enables observation of weak bands (*e.g.*, Raman overtones) close to much more intense signals. Here we show that, at moderate readout rates, the relative performances of the two detector types are not substantially different. We anticipate that sCMOS based cameras will find application for bright spectroscopies, such as multiplex CARS, as well as spontaneous Raman spectroscopy, and Raman spectral imaging.

Introduction

Electron Multiplied Charge Coupled Devices (EM-CCDs) are the current standard in low light spectroscopy and imaging. Weak signals can be detected due to the high quantum efficiency and low readout noise provided by modern deep cooled CCDs. EM gain allows for amplification of weak signals under low light conditions and enables spectral acquisition at fast readout rates by increasing the contrast between signal and noise.¹ However, the finite readout time of CCDs ultimately limits the frame rates that can be achieved.² This readout limitation has pushed high light techniques, such as stimulated Raman spectroscopy, to the use of PMTs or photodiode arrays,³ or multi-channel lock-in detection.⁴ An additional consideration here is their dynamic range: CCD detectors saturate rapidly with high intensity signals, combined with the local oscillator, or background, which overlaps the signal.

The finite readout time for CCDs is in part due to the coupled pixels on the chip architecture: all the information in a column passes through a single pixel during readout. This readout mode can result in artefacts. Information passes through pixels that might still be under illumination, which can result in streaks appearing on images.⁵ It is possible to shutter during readout, but this further decreases attainable framerates. The readout artefacts can be avoided by using an array of point detectors, which can be read out individually.⁶

The complementary metal oxide semiconductor (CMOS) camera is an alternative detector technology to CCDs. As with CCDs, CMOS sensors contain an array of pixels on a semiconductor chip. They are less sensitive in terms of S/N than CCDs, which is why CMOS sensors have not seen as much use in spectroscopy to date. However, the recent advent of scientific CMOS (sCMOS) sensors with lower noise has opened possibilities for the use of CMOS sensors in spectroscopy. Furthermore, CMOS chips do not need to be cooled to low temperatures and offer much faster readout rates compared to CCDs. Whereas CCDs are read out by stepwise transfer of charge from pixel to pixel to the readout region, in CMOS sensors each pixel is readout directly and independently. This difference in readout mechanisms avoids smearing and blooming in CMOS detectors. Avoiding these effects reduces the need for shuttering during sensor readout, further increasing achievable frame rates,⁷ especially during spectral imaging.⁵ Indeed, these differences, together with lower cost, have led to the application of CMOS sensors already in many fields such as imaging and consumer products, and in bright light applications such as UV/vis absorption spectroscopy. The lower readout noise achieved in the latest generation of sCMOS sensors is such that they may also be useful in low light and fast (microsecond to second) time resolved spectroscopic applications also.

In this contribution, we focus on the relative performance of an EM-CCD and an sCMOS detector in multiplex coherent anti-Stokes Raman scattering (mCARS) and additionally linear Raman spectroscopy. For mCARS, we focus on the spectrum of a polystyrene bead reference sample and compare limits of detection in regard to exposure times. We discuss how the quality of the spectra obtained is affected by differences in dynamic range between the two sensor types and compare and contrast accumulation time and spectral averaging approaches to increase signal to noise. Finally, we show limitations as well as an appropriate operating window for the sCMOS detector in mCARS applications. Furthermore, we show that the differences between detector performances hold for nanosecond and CW excitation, and that despite the low QE in the NIR region, the absence of interference from fringing leads potentially to an overall increase in spectral quality with sCMOS compared to NIR enhanced CCDs.

Experimental

A Kymera 193 spectrograph was equipped with and 300 l/mm, 850 nm blaze grating and both a Newton EM-CCD (DU970P-FI, cooled to -60 °C) and a Zyla 4.2 sCMOS detector (Andor Technology, UK). The sCMOS was set to 200 MHz low noise readout. A flipper mirror inside the spectrograph allowed for direct comparison between the two detectors performance by switching the beam path using the mirror, Figure 1. CW spontaneous Raman spectra were recorded at 532 nm (Cobolt Samba 300 mW) using a Shamrock-300i spectrograph equipped with and 1200 l/mm, 500 nm blaze grating and both a Newton EM-CCD (DU970P-BU, cooled to -70 °C) and a Zyla 4.1 sCMOS detector (Andor Technology, UK).

We used multitrack readout of 100 pixels to reduce vertical shift time for the CCD and multitrack readout on the sCMOS camera to reduce readout noise.

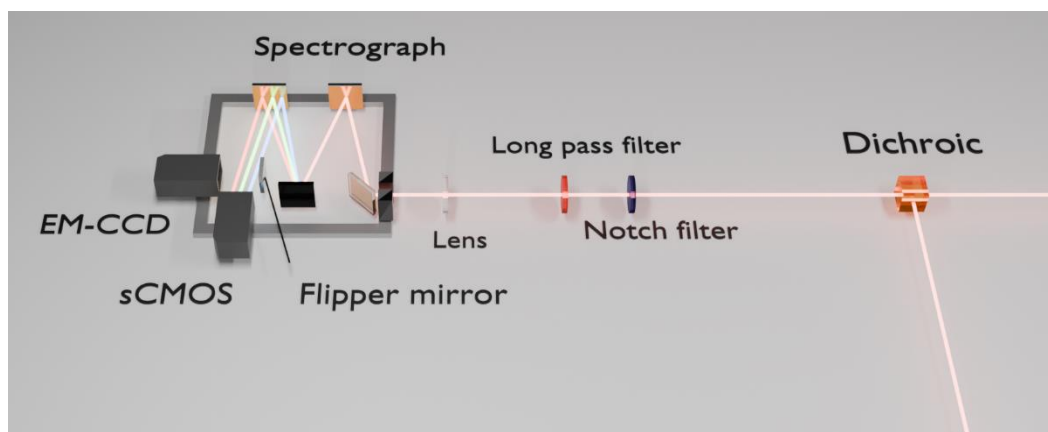


Figure 1: Optical path of the CARS signal into the spectrograph equipped with both the EMCCD and sCMOS cameras in the current study.

The CARS spectra were generated using a homebuilt broadband CARS microscope, equipped with an OPERA HP dual-output fiber laser (LEUKOS, France), delivering synchronized pump and Stokes beams with 50 ps pulse duration and 1 MHz repetition rate. The pump radiation had a wavelength of 1064 nm, while the Stokes spectrum was an infrared supercontinuum in the range 1100-1800 nm. Both beams were merged and directed onto the sample via an objective (CFI Plan Apo 60x NA 1.27, water-immersion, Nikon Corporation, Japan), with a total average power at the sample of 215 mW. The signal was collected in forward scattering mode, collimated using a second objective and directed to the spectrograph using gold mirrors. The CARS microscope is described in detail elsewhere.¹ The Raman spectra were recorded using 10 micron diameter polystyrene beads as sample. Continuous wave reference spectra were recorded on cyclohexane with a similar power at the sample (244 mW). For spontaneous Raman spectroscopy a 1 cm pathlength cuvette was used. The samples used are both standard reference materials.⁸

Results

The mCARS spectra of polystyrene beads were generated as described earlier.¹ The optical collection path is common for both EMCCD and sCMOS cameras except for the final flipper mirror in the spectrograph. The cameras were mounted to ensure that the optical plane of the spectrograph was common for both. The sCMOS QE drops steeply in the infrared region, where spectra are collected with 1064 nm pumped CARS spectroscopy, compared with NIR enhanced (back thinned) EM-CCDs used typically. For comparison, and to avoid potential interference from fringing, the EM-CCD with an open electrode sensor was chosen to match best the spectral responsivity with that of the sCMOS camera.

A significant factor in comparison, however, is the difference in both chip format (height/width) and pixel dimensions between the EM-CCD (1600 w 400 h pixels, 16 micron) and sCMOS (2048 x 2048 pixels, 6.5 micron) sensors used. The heights of the chips differ substantially, however, in point illumination, this difference is not of consequence. In contrast, the difference in pixel size means that the light gathered by each pixel differs, with the area of each pixel of the EM-CCD six times that of the sCMOS. However, in spectral mode (with binning of columns of pixels) the difference is in principle reduced to ca. three times. Due to the individual readout of pixels in sCMOS cameras, the readout noise is also three times as a result. Furthermore, the smaller pixel size of the sCMOS means that despite having a greater number of pixels in the width, the overall width of the sensor is less than that of the EM-CCD (13.3 mm vs 25.6 mm) and hence the spectral range is less. With the grating used, the entire spectrum of polystyrene can be acquired with the EM-CCD, but only half the spectrum could be

obtained with the sCMOS camera. Two halves of a spectrum were therefore stitched together using the 1614 cm^{-1} band of polystyrene, Figure 2. Normalization on this band shows comparable signal-to-noise ratios for 500 ms exposures on the sCMOS camera, vs 100 accumulations of 5 ms exposures on the EM-CCD camera, approximating the same total exposure time. The EM gain used to obtain such an increased signal also increases the noise. Furthermore, normalization on this relatively centered band shows the difference in the wavelength dependence of the quantum efficiency drop off for each detector type. Quantum efficiency drops rapidly in the NIR for both sCMOS and front illuminated CCDs and although QE is comparatively higher for the sCMOS camera in the 3000 cm^{-1} region of the CARS spectrum, overall the wavelength dependence of QE is comparable.

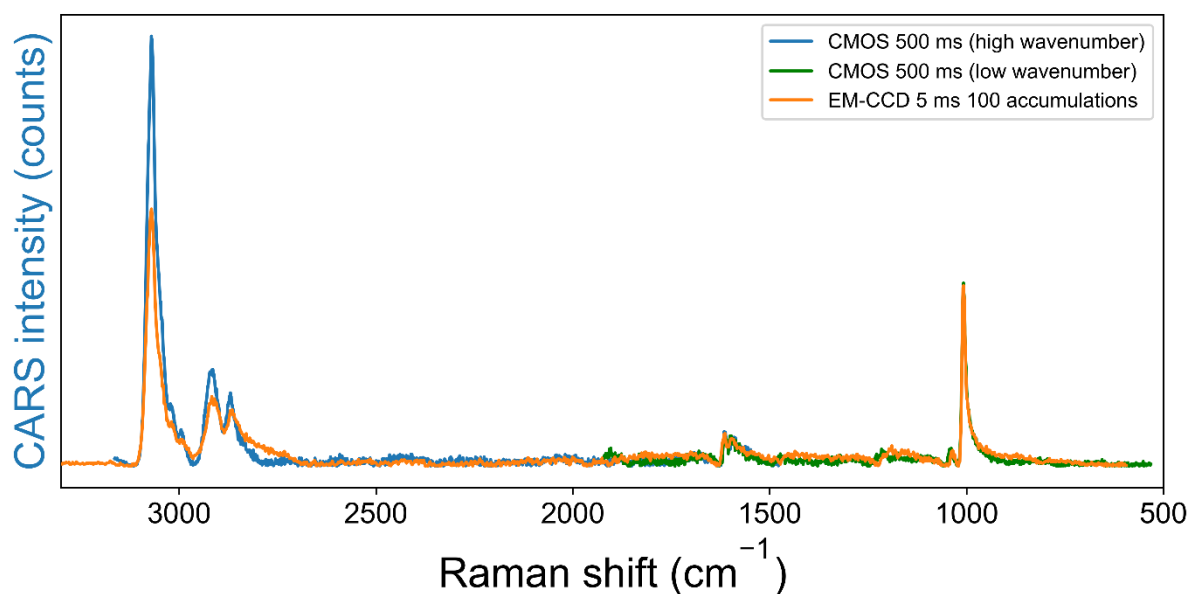


Figure 2: CARS spectra of a polystyrene bead measured on a EMCCD with 100 accumulations of 5 ms, compared to spectra measured using an sCMOS detector using a single 500 ms exposure. High- and low wavenumber spectra are normalized and stitched together using the band at 1614 cm^{-1} .

Limit of detection

Limit of detection is a common means of evaluating performance in spectroscopy. In this comparison, the limit was found by reducing readout rates. This method of comparison is especially interesting in the current case, as EM-CCD cameras are applied primarily for low light conditions, while sCMOS cameras perform well when fast readouts under bright light illumination conditions are desired.

The EM-CCD performs best in terms of signal to noise. However, the 5 ms exposure time is at the limit of CCD detectors in terms of speed. At this exposure duration, the sCMOS camera could also detect the C-H stretching bands of polystyrene, Figure 3.

The CCD exposure can be reduced, but due to the finite time of readout on CCD sensors, where pixels are still illuminated during readout, the effective exposure time does not change. Physical shuttering during readout can prevent this extra exposure, at the cost of further decreased frame rates. sCMOS does not have this limitation, as it reads out each pixel individually, with rates up to 25 kHz and therefore, with sufficient light intensity, the sCMOS detector can be read out faster (*vide infra*).

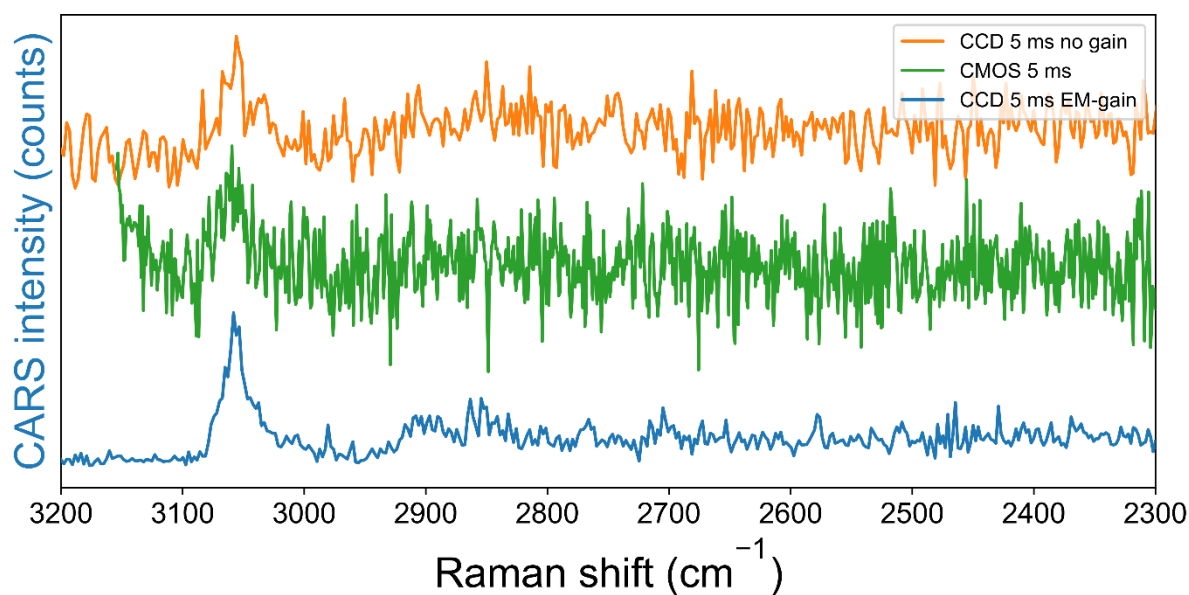


Figure 3: Spectra recorded under identical optical and sample conditions by a sCMOS, EMCCD without gain (CCD mode) and EM-CCD with maximum gain. Normalized on the 3055 cm^{-1} aromatic CH stretching band of polystyrene. Spectra are offset on the y-axis for clarity. The 3055 cm^{-1} band is observed in all three spectra, with the best S/N ratio in the spectrum acquired using the EMCCD with EM gain. 5 ms was chosen as this the fastest spectral rate achievable with the EM-CCD.

Dynamic range

Increasing the signal to noise ratio is desirable over speed where higher quality spectra are required. However, in bright, high background conditions such as CARS spectroscopy, long exposures on a CCD type detector are often not feasible. The onset of saturation as a result of the dynamic range of CCD chips (*well depth is* 2^{16}) results in unusable spectra when the exposure is too long. Spectra become unusable because the flatline at the maximum well depth extends beyond the illuminated pixels under such conditions. In such cases, the signal blooms to nearby pixels which obscures the spectrum. Generally, multiple short exposures are averaged to a single spectrum to overcome the low dynamic range, *e.g.*, when saturation is reached with a single 500 ms exposure, accumulation of shorter exposures, such as one hundred 5 ms exposures as shown in Figure 2 (*vide supra*).

sCMOS sensors are as sensitive in terms of QE, however the readout noise is more pronounced as pixels are readout individually. Especially under low light conditions such as short exposures the s/n ratios achievable are lower than with a CCD sensor. An obvious approach to increase spectral quality is to average or sum several acquisitions, similar to the approach taken with CCD cameras. However, this approach does not yield the same benefits due to the readout noise, meaning that even though the absolute readout noise may be low, it is a constant factor for each pixel, and is not reduced effectively by averaging, as the charge does not pass through a readout-register such as in CCD detectors. Therefore, the overall noise level stays relatively equal, and different for each pixel, even after accumulation of several exposures under low-light exposures. This finite readout noise results in only marginal improvements with one hundred acquisitions versus only one longer acquisition using a sCMOS camera, Figure 4. Increasing the exposure time is a better approach as saturation is less easily reached as the pixel well depth on the sCMOS chip, and thus the dynamic range, is much larger compared to CCD, due to 4 pixels being read out together. This readout results in an equivalent area on the chip compared to the CCD (one 13 micron pixel vs four 6.5 micron pixels). The comparison in

Figure 4 shows the improved and signal to noise ratio between a single 500 ms exposure and one hundred 5 ms exposures.

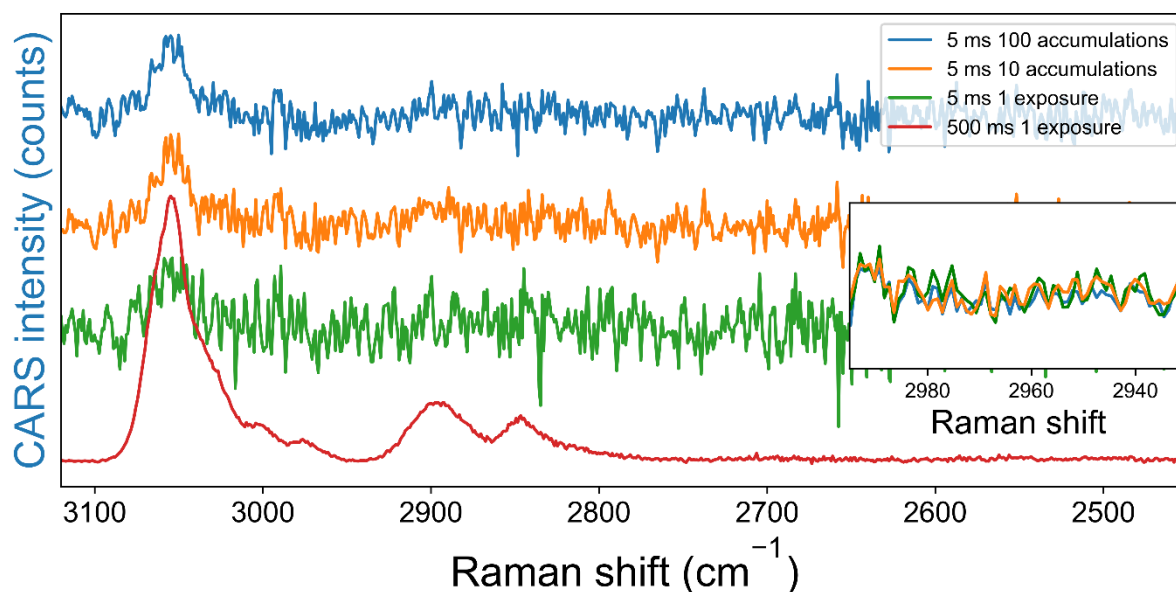


Figure 4: CARS spectra of a polystyrene bead at 5 ms exposure and multiples of accumulations thereof, compared to a single shot of 500 ms exposure. Spectra recorded with an sCMOS camera. Inset: baseline zoomed in to show the equivalent readout-noise pattern obtained after multiple accumulations.

The dynamic range of sCMOS sensors can be much larger compared to CCD chips, due to the difference in read out mode. The sCMOS chip has on-chip readout of 4 pixels binned together ($4 \times 2^{16} = 2^{18}$). Additionally, the size of the pixels is roughly six times smaller, so fewer photons are collected per pixel for the same exposure. Finally, signal blooming is much less pronounced on sCMOS chips. Indeed, exposures can be significantly longer without saturation for the same light intensity, Figure 5. Because of the difference in readout mode, the rate of signal acquisition seems to decrease over longer exposures. The cause of this effect is the four pixels binned together (vide supra). One of the four might be more in focus of the signal and thus can fill already before the end of the exposure, while the other three continue to fill. This difference in rate means general spectral shapes are maintained near saturation, in contrast to CCDs, which give a constant output when saturated. The background also increases with these overexposures on the sCMOS, however, bands of interest are still relatively undistorted.

The high dynamic range and nonlinear dependence on the signal intensity allows longer exposure to detect weak bands that sit close to intense bands by exposing longer without saturation. This characteristic is useful, especially, in broadband CARS, where the weak fingerprint bands are ideally obtained by long exposures, however, CCD cameras tend to saturate by intense CH stretching bands. This advantage of sCMOS detection becomes apparent, *e.g.*, for the smaller bands between 3000 and 3055 cm^{-1} , which are not clearly observable with shorter exposures.

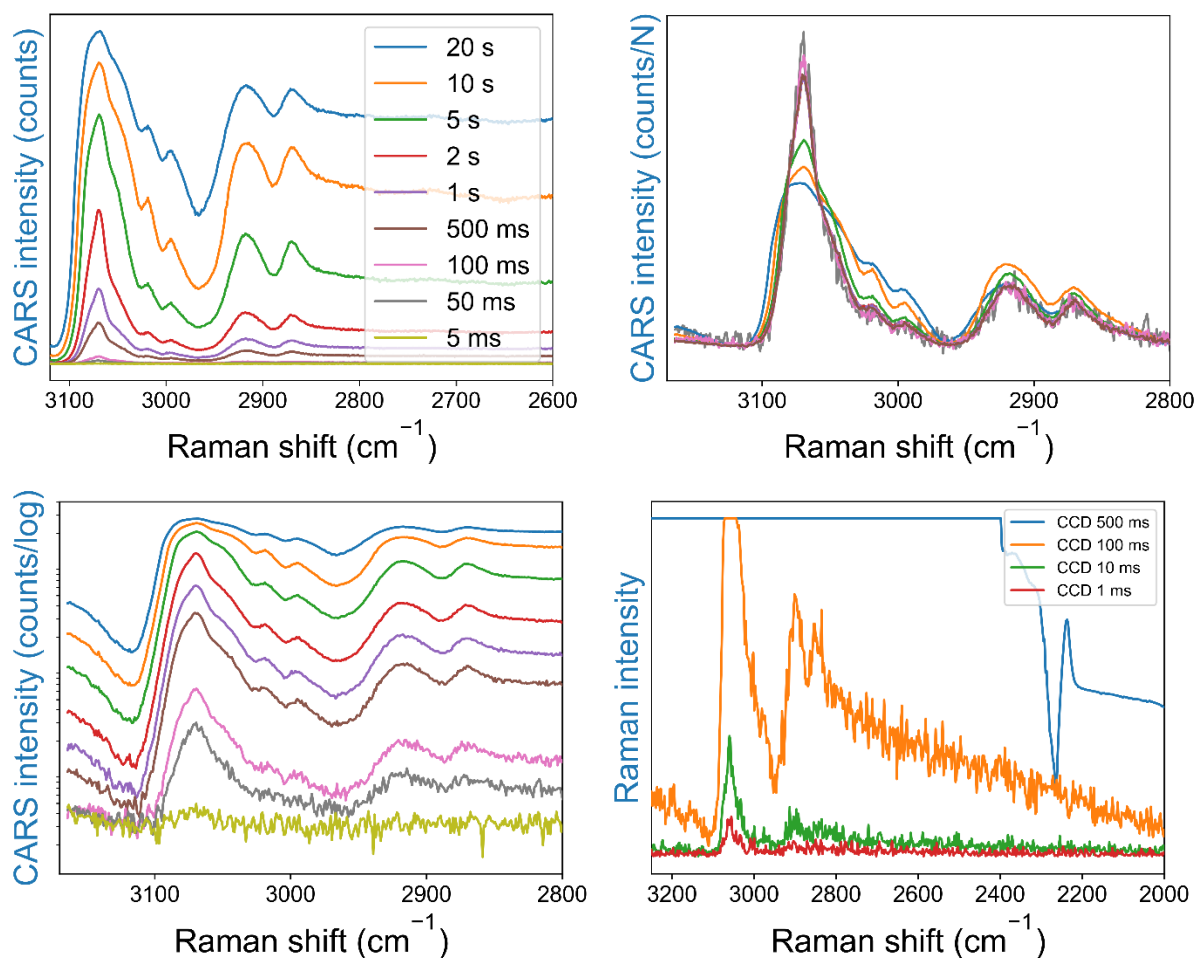


Figure 5: CARS spectra of a polystyrene bead recorded at various exposure times on a sCMOS and CCD detector. (top, left) Raw sCMOS data. (top, right) sCMOS Normalized on the 3055 cm^{-1} band of PS. (bottom, left) sCMOS logarithmic scaled data. (bottom, right) Raw CCD data.

The difference and drawback with these overexposures is the loss of resolution, as the center of the bands increases less quickly than the sides. The result is a thicker band. The full width at half maximum (FWHM) is a measure for the spectral resolution, and is plotted against the signal to visualize differences over time, and, visualize optimal exposure times, Figure 6. The x axis indicates a broad range of usable exposure times from 5 ms to 20 s. This dynamic range is much larger than can be expected for CCD sensors and is within reasonable acquisition rates for spectroscopy and spectral imaging. Additionally, the signal intensity is linear between 5 ms and 2 s, before the onset of the broadening effect. Significant increases of the FWHM are only observed after 2 s exposures. We observe a similar result for Raman signals measured using a continuous wave laser source, Figure S1 and S2.

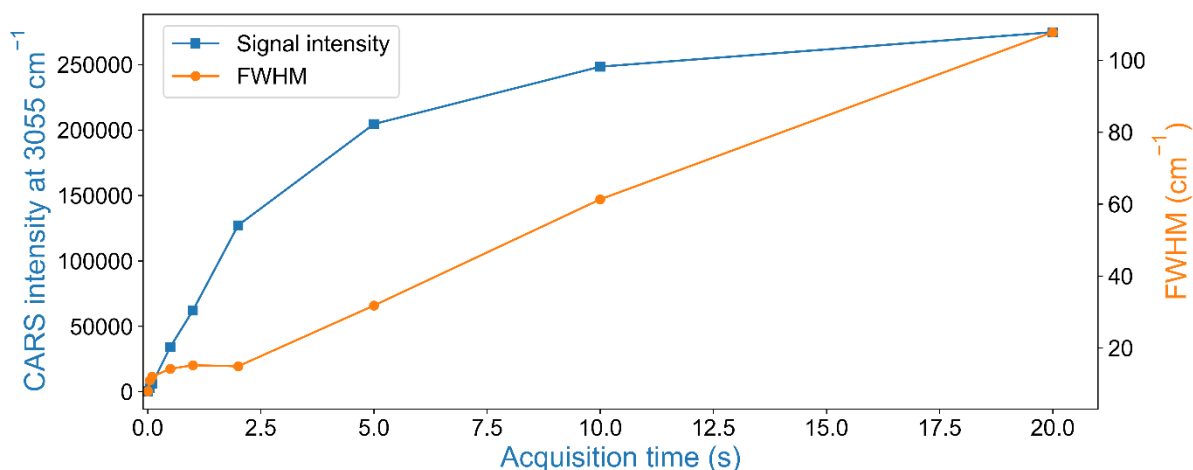


Figure 6: Extracted signal and FWHM values from Figure 5. Between 50 ms and 2 s the sCMOS has relatively high signal to noise ratios as well as good spectral resolution.

Conclusion

The EM-CCD and sCMOS detectors with similar performance. In terms of QE in sCARS, and nanosecond and continuous wave linear Raman spectroscopy were compared using a polystyrene bead reference sample and cyclohexane, respectively. At low light, relatively fast readout rates EMCCD still outperforms the sCMOS chip. However, the finite readout time is becoming a limitation for the CCD. sCMOS does not have this limitation and indeed can read out faster (e.g., figure S3), although it is not yet sensitive enough to do. The sCMOS is still limited by a relatively higher readout noise and lower sensitivity, in particular in low light conditions.

We anticipate that the sCMOS will find increased use in spectroscopy and Raman spectral imaging as improvements in the technology continue. In particular, bright and coherent spectroscopies could benefit from the high readout rates already, given their relatively high signal intensities. Furthermore, the large dynamic range of the sCMOS, combined with the generally lower cost, could make them useful alternatives for expensive CCD detectors in non-spectroscopy centered applications such as bio-imaging.

Bibliography

- (1) Murakami, Y.; Yoshimura, M.; Niels Klement, W. J.; Oda, A.; Sakamoto, R.; Yakabe, M.; Matsumoto, A.; Oketani, R.; Leproux, P.; Ikenouchi, J.; Browne, W. R.; Kano, H. Backward Multiplex Coherent Anti-Stokes Raman (CARS) Spectroscopic Imaging with Electron-Multiplying CCD (EM-CCD) Camera. *Opt. Continuum* **2023**, 2 (9), 2044. <https://doi.org/10.1364/OPTCON.497869>.
- (2) Kizawa, S.; Hashimoto, M. Ultrahigh-Speed Multiplex Coherent Anti-Stokes Raman Scattering Microspectroscopy Using Scanning Elliptical Focal Spot. *The Journal of Chemical Physics* **2021**, 155 (14), 144201. <https://doi.org/10.1063/5.0063987>.
- (3) Lin, H.; Lee, H. J.; Tague, N.; Lugagne, J.-B.; Zong, C.; Deng, F.; Shin, J.; Tian, L.; Wong, W.; Dunlop, M. J.; Cheng, J.-X. Microsecond Fingerprint Stimulated Raman Spectroscopic Imaging by Ultrafast Tuning and Spatial-Spectral Learning. *Nat Commun* **2021**, 12 (1), 3052. <https://doi.org/10.1038/s41467-021-23202-z>.

- (4) De La Cadena, A.; Vernuccio, F.; Ragni, A.; Sciortino, G.; Vanna, R.; Ferrante, C.; Pediconi, N.; Valensise, C.; Genchi, L.; Laptенок, S. P.; Doni, A.; Erreni, M.; Scopigno, T.; Liberale, C.; Ferrari, G.; Sampietro, M.; Cerullo, G.; Polli, D. Broadband Stimulated Raman Imaging Based on Multi-Channel Lock-in Detection for Spectral Histopathology. *APL Photonics* **2022**, *7* (7), 076104. <https://doi.org/10.1063/5.0093946>.
- (5) Klement, W. J. N.; Savino, E.; Browne, W. R.; Verpoorte, E. In-Line Raman Imaging of Mixing by Herringbone Grooves in Microfluidic Channels. *Lab Chip* **2024**, *24* (14), 3498–3507. <https://doi.org/10.1039/D4LC00115J>.
- (6) Nitta, N.; Iino, T.; Isozaki, A.; Yamagishi, M.; Kitahama, Y.; Sakuma, S.; Suzuki, Y.; Tezuka, H.; Oikawa, M.; Arai, F.; Asai, T.; Deng, D.; Fukuzawa, H.; Hase, M.; Hasunuma, T.; Hayakawa, T.; Hiraki, K.; Hiramatsu, K.; Hoshino, Y.; Inaba, M.; Inoue, Y.; Ito, T.; Kajikawa, M.; Karakawa, H.; Kasai, Y.; Kato, Y.; Kobayashi, H.; Lei, C.; Matsusaka, S.; Mikami, H.; Nakagawa, A.; Numata, K.; Ota, T.; Sekiya, T.; Shiba, K.; Shirasaki, Y.; Suzuki, N.; Tanaka, S.; Ueno, S.; Watarai, H.; Yamano, T.; Yazawa, M.; Yonamine, Y.; Di Carlo, D.; Hosokawa, Y.; Uemura, S.; Sugimura, T.; Ozeki, Y.; Goda, K. Raman Image-Activated Cell Sorting. *Nat Commun* **2020**, *11* (1), 3452. <https://doi.org/10.1038/s41467-020-17285-3>.
- (7) Chang, K.-Y. CMOS SENSOR. US6207984.
- (8) ASTM. Standard Guide for Testing the Resolution of a Raman Spectrometer. <https://doi.org/10.1520/E2529-06R14>.